doi:10.1111/evo.12995

Trends in the sand: Directional evolution in the shell shape of recessing scallops (Bivalvia: Pectinidae)

Emma Sherratt,[1,2,3] Alvin Alejandrino,[1] Andrew C. Kraemer,[1] Jeanne M. Serb,[1,*] and Dean C. Adams[1,4,*]

[1]*Department of Ecology, Evolution, and Organismal Biology, Iowa State University, Ames, Iowa 50011*

[2]*Division of Evolution, Ecology and Genetics, The Australian National University, Canberra, ACT 2601, Australia*

[3]*E-mail: emma.sherratt@gmail.com*

[4]*Department of Statistics, Iowa State University, Ames, Iowa 50011*

Received December 28, 2014
Accepted June 21, 2016

Directional evolution is one of the most compelling evolutionary patterns observed in macroevolution. Yet, despite its importance, detecting such trends in multivariate data remains a challenge. In this study, we evaluate multivariate evolution of shell shape in 93 bivalved scallop species, combining geometric morphometrics and phylogenetic comparative methods. Phylomorphospace visualization described the history of morphological diversification in the group; revealing that taxa with a recessing life habit were the most distinctive in shell shape, and appeared to display a directional trend. To evaluate this hypothesis empirically, we extended existing methods by characterizing the mean directional evolution in phylomorphospace for recessing scallops. We then compared this pattern to what was expected under several alternative evolutionary scenarios using phylogenetic simulations. The observed pattern did not fall within the distribution obtained under multivariate Brownian motion, enabling us to reject this evolutionary scenario. By contrast, the observed pattern was more similar to, and fell within, the distribution obtained from simulations using Brownian motion combined with a directional trend. Thus, the observed data are consistent with a pattern of directional evolution for this lineage of recessing scallops. We discuss this putative directional evolutionary trend in terms of its potential adaptive role in exploiting novel habitats.

KEY WORDS: **Directional evolution, geometric morphometrics, mollusca, pectinidae.**

Determining the path, or manner of phenotypic change in morphospace is a major goal in macroevolution (Simpson 1944; Sidlauskas 2008; Scannella et al. 2014). One of the most compelling evolutionary patterns observed in paleontological sequences are persistent, directional changes, or evolutionary trends (McKinney 1990; Knouft and Page 2003; McNamara 2006). The identification of directional trends has long been a focal point of macroevolutionary studies (e.g., Osborn 1929; Simpson 1944; Wagner 1996; MacFadden 2005), and inferring the processes responsible for such trends is also of considerable interest (Vermeij 1987; Gould 1988; McShea 1994; Alroy 2000). Some classic examples of directional trends include increasing body size and shifts in tooth dimensions of horses (MacFadden 1986, 2005), increased body segmentation and complexity in trilobites (Sheldon 1987; Fortey and Owens 1990), and increased horn size in titanotheres (Osborn 1929; Bales 1996). Indeed, the tendency for many clades to increase in body size over time (Cope's rule) is perhaps the most commonly cited example of an evolutionary trend (Cope 1896; Rensch 1948; Alroy 1998), though the causes of these body size trends are still not fully understood (Hone and Benton 2005; Heim et al. 2015).

Much research on the evolution of directional trends has focused on whether such patterns are the result of adaptation and processes such as directional selection, or whether random diffusion is sufficient to explain directional patterns (see McShea 1994). Surprisingly, differentiating between randomly and

*These authors joint last author.

EVOLUTION
INTERNATIONAL JOURNAL OF ORGANIC EVOLUTION

nonrandomly generated trends has often proved challenging (Alroy 2000). For example, theoretical work has demonstrated that for ancestor-to-descendent (allochronic) sequences, it is often difficult to refute the null model of a random walk when comparing it to the alternative of a directional trend (Bookstein 1987; Bookstein 1988; Roopnarine et al. 1999; Sheets and Mitchell 2001; and see also Bookstein 2013). Empirically, several meta-analyses summarizing empirical patterns in hundreds of fossil sequences have indicated that only a small percentage of cases actually represent directional evolution; in the vast majority of cases, patterns of change cannot be statistically differentiated from patterns expected under models of Brownian motion (BM) or stasis (Hunt 2007; Hopkins and Lidgard 2012). Thus, despite the focus of macroevolutionary studies on directional evolution, both theoretical and empirical surveys suggest that directional change in evolution may in fact be quite rare.

In paleontological studies, directional trends are frequently quantified by calculating the phenotypic differences (i.e., distance) from time step to time step in allochronic sequences, then modeling the distribution of these changes relative to what is expected under random walk and directional models (e.g., Bookstein 1987; Hunt 2006). Likewise, for a set of extant species, phenotypic changes along a phylogeny are regressed against node rank or phylogenetic distance to identify directional patterns (Pagel 1997; Knouft and Page 2003; Poulin 2005; Verdú 2006; Bergmann et al. 2009). These methods are for single traits such as body size or some composite measure (i.e., principal component scores). While extensions of some of these methods have been used with multivariate data along allochronic sequences (Wood et al. 2007), these methods have not been applied in a phylogenetic context. Furthermore, generalizing existing approaches to their multivariate counterparts can be challenging, because while univariate changes, represented as either independent contrast scores or as changes from ancestral to descendent nodes, confer directional information by way of sign change, multivariate changes from time step to time step are vectors that encode both a magnitude and a direction of change (see Klingenberg and Monteiro 2005; Adams and Collyer 2009; Collyer and Adams 2013). Thus, for multivariate phenotypes one must mathematically disentangle the amount (magnitude) of evolutionary change from the direction of those changes in morphospace, so that putative directional trends may be properly evaluated.

Fortunately, multivariate data and the patterns of phenotypic variation it represents may be directly visualized in a morphological trait space (or morphospace, sensu Raup 1966). Further, when phylogenetic information is available, estimates of ancestral states may be included and the phylogeny projected into morphospace, resulting in a phylomorphospace (Rohlf 2002; Sidlauskas 2008). Importantly, phylomorphospaces provide a surprisingly simple means of identifying putative evolutionary trends, because it yields both a visualization of patterns of morphological variation, as well as insights into the path of phenotypic change for individual lineages. For example, patterns of parallel evolution are readily identified by branches on the phylogeny that traverse morphospace in similar directions, whereas convergent evolution is found when terminal taxa are more similar in their locations in morphospace than are their immediate ancestors (Stayton 2006; Revell et al. 2007). Furthermore, the interpretation of a clade's dispersion pattern in morphospace (equating to morphological disparity) is greatly enhanced by examining how branches spread through this space (e.g., Sidlauskas 2008; Hopkins 2016). We contend that this simple visual approach also provides a means of identifying putative patterns of directional evolutionary trends in highly multivariate phenotypes. In this case, patterns of phenotypic change along a phylogeny will manifest as a sequence of ancestor and descendent species, aligned one after another along a common trajectory, traversing morphospace in a similar direction. We further propose that by combining this visualization with simulation-based comparisons of phenotypic variation under alternative evolutionary scenarios (see below), patterns of directional evolution of high-dimensional phenotypes may be identified relative to alternative processes, such as pure Brownian motion.

In this study, we quantify patterns of shell shape evolution in scallops. Bivalved scallops (Pectinidae) are a particularly good system to study evolutionary patterns of morphological change: they are a geographically wide-ranging, speciose clade displaying an array of shell morphologies. Because shell shape reflects the ecology ("life habit") of the animal (Stanley 1970), adult scallops can be broadly organized into six functional groups that vary in their level of mobility (cementing, nestling, byssal attaching, recessing, free-living, and long-distance swimming: Stanley 1970; Alejandrino et al. 2011). We use geometric morphometrics and phylogenetic comparative methods to infer the history of morphological diversification in shell shape across species. We identify that morphospace is partitioned by distinct shell shapes of these six life habits. We also identify a distinct, directional phylogenetic trend in shell shape among species that have a recessing life-habit, and evaluate this pattern using phylogenetic simulations (sensu Pennell et al. 2015).

Materials and Methods

SAMPLES

We sampled 844 adult individuals from 93 species (average 8.9 individuals per species, details in Table S1), covering the breadth of morphological and ecological diversity in the Pectinidae. Scallops display six distinct behavioral habits that vary in their degree of activity (Table 1). Our dataset spanned the range of behavioral habits exhibited in scallops, and contained representative species

Table 1. Descriptions of predominant behavioral habits of scallops.

Behavioral habit	Description	References
Cementing	Permanently attaches to hard or heavy substratum by right valve	Waller 1996
Nestling	Settle and byssally attaching to living *Porites* corals; coral grows around scallop	Yonge 1967
Byssal-attaching	Temporarily attaches to a substratum by byssus threads; can release and reorientate	Brand 2006
Recessing	Excavates cavity in soft sediment; full/partial concealment	Baird 1958; Sakurai and Seto 2000
Free-living	Rests above soft sediment or hard substratum	Stanley 1970
Long-distance swimming ("gliding")	Able to swim >5 m/effort; includes a level swimming phase with a glide component	Chang et al. 1996; Brand 2006

from each group. Briefly, these behavioral habit groups are described as follows. Cementing species, which attach permanently to hard substrate as adults, are represented here by *Crassadoma gigantea* and *Talochlamys pusio*. Nestling behavior involves settling, byssally attaching, and becoming embedded in living corals, and is represented by a single species, *Pedum spondyloideum*. Byssal attachment, the most-common life habit of scallops, involves a temporary attachment to substratum by byssus threads. Our sample includes 53 byssal species. Recessing behavior involves excavating a cavity in soft sediment, resulting in full or partial concealment (but no attachment). This habit is represented here by species from two clades, the *Euvola* group (ten spp.) and *Patinopecten* group (two spp.); the clades are herein named simply by a single genus for brevity, but they comprise three and two genera respectively. Free-living species, the second most-common behavior, involves resting on soft or hard substrates without any attachment, and our sample includes 19 species. Finally, we have seven species of the most active behavior, gliding, where the scallop swims by jetting water from gaps along the dorsal shell margin while the valves are held closed. All species were sampled from museum collections (Table S1). This dataset includes specimens examined previously by Serb et al. (2011).

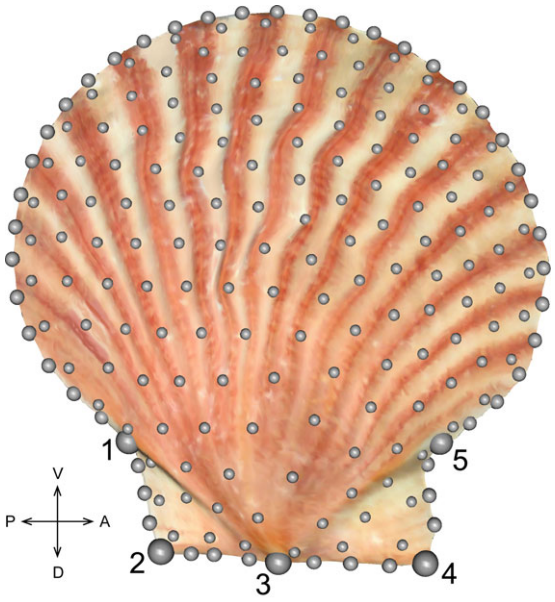

Figure 1. A three-dimensional surface scan of the left valve of a representative scallop with the landmarks and semilandmarks indicated. Five landmarks are numbered and represented by large dots and the semilandmarks are shown as small dots. Landmark 1: ventroposterior auricle, 2: dorsoposterior auricle, 3: umbo, 4: dorsoanterior auricle, 5: ventroanterior auricle.

MORPHOMETRIC ANALYSES

Shell shape was characterized using landmark-based geometric morphometrics (Bookstein 1991; Mitteroecker and Gunz 2009; Adams et al. 2013). We used a combination of fixed landmarks representing homologous points and semilandmarks, points on curves and surfaces (Gunz et al. 2005; Mitteroecker and Gunz 2009). First, we obtained three-dimensional surfaces representing the left valve using a NextEngine 3D scanner (Next Engine Inc., Santa Monica, CA). On this surface, we placed 202 landmarks to cover the boundary contours of the valve, auricles and umbo, as well as the curvature of the valve in the z dimension (Fig. 1). Of these landmarks, five were fixed, "type 1" landmarks (sensu Bookstein 1991) demarcating homologous points on the auricles and umbo following Serb et al. (2011). Between each of these fixed points, three equally spaced sliding semilandmarks were digitized on the boundary to capture the shape of the auricles (12 in total). Around the boundary we digitized 35 equally spaced sliding semilandmarks to capture the shape of the valve. Finally, 150 semilandmarks were fit to the shell surface using a template, and these are allowed to slide in 3D over the surface. For this we produced a template mesh on a single specimen, and used the thin-plate spline to warp this template to the surface of a second specimen. The common set of fixed points and edge landmarks

between the template and the specimen were used as the basis of this warping. Then, the remaining template points were matched to the specimen scan and the surface points nearest to those in the template were treated as surface semilandmarks for that specimen. Digitizing routines were written in R v.3.1.0 (R Development Core Team 2014) modified from those in the *geomorph* library (Adams and Otárola-Castillo 2013). The landmark scheme differs slightly from Serb et al. (2011); the number of surface landmarks was reduced, the number of shell boundary semilandmarks increased, and twelve semilandmarks were added around the auricles.

Each valve was measured twice to account for digitizing measurement error. The landmark data from both datasets were aligned using a generalized Procrustes superimposition (Rohlf and Slice 1990). The semilandmarks were permitted to slide along their tangent directions in order to minimize Procrustes distance between specimens (Gunz et al. 2005). Specifically, semilandmarks along the shell boundary edges were allowed to slide either direction in one plane, and semilandmarks on the shell surface slid in either direction on two planes. Finally, the resulting Procrustes shape coordinates were averaged per specimen, and used as shape variables in the subsequent analyses.

PHYLOGENETIC ANALYSES

To examine the shell shape variation in a phylogenetic context, we constructed a robust, time-calibrated phylogeny using all molecular data available (Fig. S1). Sequence data for two mitochondrial genes (12S, 16S ribosomal RNAs) and two nuclear genes (histone H3, 28S ribosomal RNA) were obtained from museum specimens using procedures in Pusledniknik and Serb (2008) and Alejandrino et al. (2011). The molecular dataset contained a total of 143 species, including five outgroup taxa (Table S2). Sequence data were aligned using CLUSTAL W (Thompson et al. 1994) in Geneious Pro v.5.6.4 (http://www.geneious.com, Kearse et al., 2012) with a gap-opening penalty of 10.00 and a gap-extending penalty of 0.20. GBlocks Server (Talavera and Castresana 2007) was used to remove ambiguous alignment in 16S rRNA. For Bayesian inference, we used a relaxed clock model as implemented in BEAST v.1.8.0 (Drummond and Rambaut 2007). This analysis used a speciation model that followed incomplete sampling under a birth-death prior, with rate variation across branches uncorrelated and exponentially distributed. Three independent simulations of Markov Chain Monte Carlo for 20 million generations were run, sampling every 100 generations, and 20,000 trees were discarded as burn-in using Tracer v.1.6 l (Drummond and Rambaut 2007). The remaining trees were combined in LogCombiner; the best tree was selected using TreeAnnotator. We used 30 fossils to constrain the age of nodes through assigning node priors, details of which are in Table 2. The phylogeny was then pruned to include only the 93 species for which we also have morphological data (Fig. 2).

COMPARATIVE ANALYSES

To estimate the evolutionary history of shell morphology, we used a phylomorphospace approach (e.g., Klingenberg and Ekau 1996; Rohlf 2002; Sidlauskas 2008). First, we estimated the ancestral shell shapes for each node on the phylogeny, using the species-average shape variables and maximum likelihood (Schluter et al. 1997). Next, the matrix of ancestral estimates was combined with the matrix of species data, and the combined dataset was subjected to a principal components analysis. Finally, to visualize patterns of shape evolution, the phylogeny was projected into the morphospace described by PC1 and PC2 (Fig. 3) (e.g., Sidlauskas 2008).

To evaluate whether shell shape differed among the life habit groups while taking phylogeny into account, we performed a phylogenetic ANOVA using a recent generalization of phylogenetic generalized least squares (PGLS) for high-dimensional multivariate data (Adams 2014b). Briefly, a linear model $\mathbf{Y} \sim \mathbf{X}\boldsymbol{\beta} + \boldsymbol{\varepsilon}$ is used, where $\mathbf{Y}$ is a $N \times p$ matrix representing the mean-centered set of dependent variables, $\mathbf{X}$ is a matrix containing the predictor variables and a column of ones to represent the intercept, and $\boldsymbol{\beta}$ is a matrix of regression coefficients, with one column for each variable and one row for each predictor column. The error of the model, $\boldsymbol{\varepsilon}$, is described by the $N \times p$ matrix of residuals, which contains the lack of independence due to the phylogeny as encoded by the phylogenetic covariance matrix $\mathbf{C}$ (under a BM model of evolution: see Adams 2014b; Adams and Collyer 2015). The approach tests the observed covariation between $\mathbf{X}$ and $\mathbf{Y}$ relative to the null hypothesis of no relationship between them (i.e., that the coefficients in $\boldsymbol{\beta}$ are equal to zero: see Adams 2014b; Adams and Collyer 2015).

The model is implemented using phylogenetic transformation (sensu Garland Jr and Ives 2000), where the $\mathbf{X}$ and $\mathbf{Y}$ data matrices are first transformed by the phylogeny, and the parameters of the model are then estimated from these transformed data matrices (for technical details see Adams 2014b). As with usual implementations of multivariate PGLS, the set of multivariate parameter estimates for the model are the same as those found from a series of univariate least-squares regressions performed separately on each column of $\mathbf{Y}$ relative to $\mathbf{X}$ (see Rencher and Christensen 2012). Sums of squares and cross-products matrices (SSCP) are identical using either the multivariate PGLS or the D-PGLS procedure (see SI for illustration).

The main difference between the two methods is in how the significance of the model is assessed. For multivariate PGLS, SSCP matrices are used to estimate multivariate test coefficients (e.g., Wilks' lambda, Pillai's trace), which are subsequently evaluated with theoretical probability distributions. However, such traditional methods require that the number of variables (p) is less than the error degrees of freedom of the model, and thus lose statistical power as p approaches N (see Adams 2014b). By

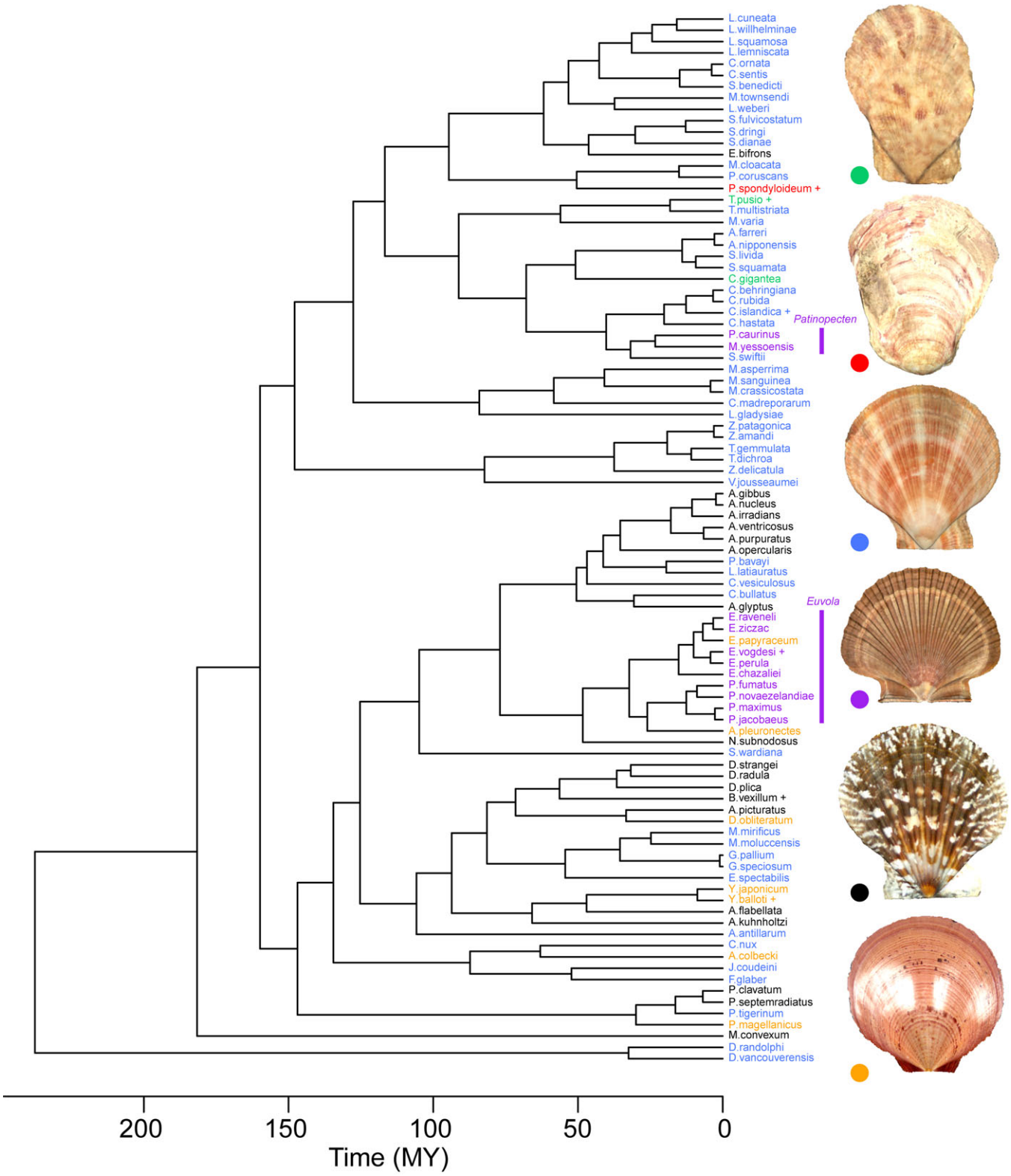

Figure 2. Chronogram of 93 scallop species. Species labels are colored by life habit (green = cementing, red = nestling, blue = byssal attaching, purple = recessing, black = free-living, orange = gliding). Left valves of example species (marked by +) are shown on the right, in order from most sessile (top) to most motile (bottom). Details of taxa in Table S1.

Table 2. Mean and standard deviation (stdev) calibration dates of stem and clade groups used to calibrate the time-tree (Fig. 2, Fig. S1).

Stem/clade	Mean date ± stdev (MY)	References
Amusium pleuronectes	28.6 ± 5.38	Hertlein 1969; Waller 1991
Euvola papyraceum	0.1 ± 0.06	Waller 1991
Pecten	12.8 ± 10.22	Waller 1991
Euvola	7.1 ± 4.51	Hertlein 1969; Waller 1991
Pecten-Euvola	25 ± 9.02	Hertlein 1969; Waller 1991
Caribachlamys mildredae	3.5 ± 0.5	Waller 1993
Caribachlamys ornata	2.2 ± 0.4	Waller 1993
Caribachlamys	3.1 ± 0.51	Waller 1993
Propeamussiidae	241.1 ± 6.1	Hertlein 1969; Waller 2006
Spondylidae	164 ± 3	Waller 2006
Pectinoidea	250 ± 2.75	Waller 2006
Pectinidae	239 ± 9	Hertlein 1969; Waller 1991
gibbus-nucleus	2.2 ± 0.4	Waller 1991
Argopecten	9.3 ± 6.69	Waller 1991
Aequipecten glyptus	4 ± 1.37	Waller 1991
Aequipecten opercularis	19.5 ± 3.53	Waller 1991
Aequipectinini	42.9 ± 4.9	Waller 1991
Spathochlamys benedicti	3.1 ± 0.52	Waller 1993
Chlamys	12.8 ± 10.22	Waller 1991
Mesopeplum convexum	8.5 ± 3.14	Beu 1978
Decatopecten	42.9 ± 4.9	Waller 1991
Equichlamys- Notochlamys	36 ± 20.02	Waller 1991
Azumapecten farreri	3.1 ± 0.51	Waller 1991
Crassadoma gigantea	17.3 ± 5.71	Waller 1993
Placopecten magellanicus	8.5 ± 3.14	Waller 1991
Laevichlamys multisquamata	2.2 ± 0.4	Waller 1993
Patinopecten -Mizuhopecten	28.6 ± 5.38	Waller 1991
Caribachlamys sentis	4.5 ± 0.87	Waller 1993
Swiftopecten swiftii	19.5 ± 3.53	Waller 1991
Mimachlamys varia	19.5 ± 3.53	Waller 1991

Dates in millions of years (MY).

contrasts, D-PGLS summarizes the fit of the model using the total residual sums of squares (SS_{resid}), found as the trace of the $SSCP_{resid}$ (i.e., the sum of SS_{resid} for each **Y**). The significance of the model is evaluated via permutation, where rows of **Y** are permuted relative to **X**, all of the above calculations are repeated, and SSCP matrices are calculated, generating a sampling distribution of SS_{resid}. Importantly, this approach retains high power even as the number of variables (p) is large relative to or exceeds the number of species (N), thereby permitting significance testing of model effects irrespective of the number of variables (Adams 2014b).

EVALUATING DIRECTIONAL TRENDS

To evaluate directional trends in a phylogenetic context, we extended an existing method for evaluating multivariate directional evolution in allochronic sequences (Wood et al. 2007) and combined it with phylogenetic simulations performed under several alternative evolutionary scenarios (sensu Pennell et al. 2015). To measure directional evolution in multivariate data obtained from allochronic sequences, Wood et al. (2007) proposed estimating the mean angular direction of phenotypic change from time-step to time-step as one summary measure. Here, we build upon Wood et al.'s procedure by devising a phylogenetic equivalent. First we used principal components and phylomorphospace to visually assess whether patterns of shape evolution in particular lineages displayed a directional trend, based on the direction of branching patterns and the position of extant species in the morphospace. Using this approach, we identified a putative directional trend in the *Euvola* clade of recessing species (see below).

Next, for the set of recessing species in the *Euvola* clade we calculated the mean pairwise angular direction (MPA) of evolution in morphospace. This was accomplished by estimating the evolutionary change vectors for all recessing species in the *Euvola* clade, which were found as the difference in shape between

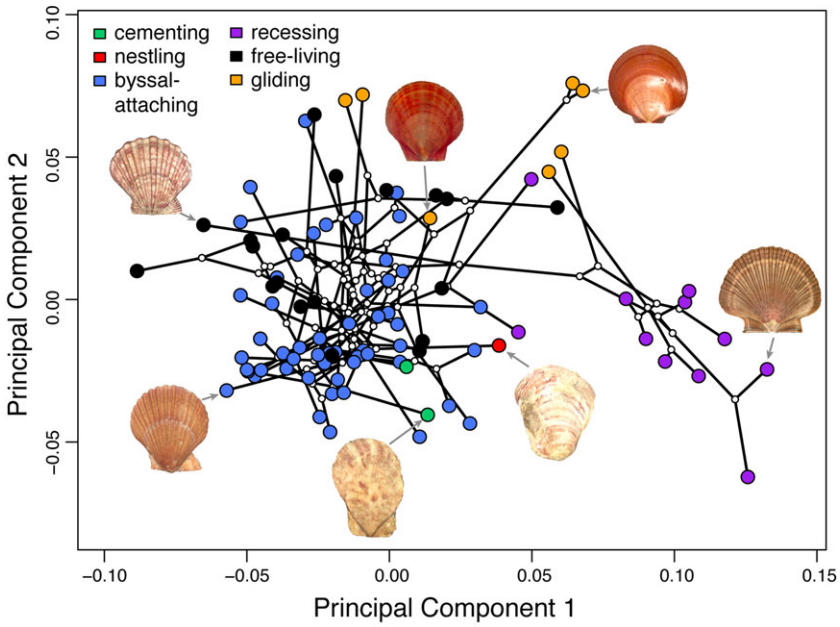

Figure 3. **Phylomorphospace of average shape for 93 species, colored by habit group (same as Fig. 2), and illustrated with example species. White circles represent ancestral states estimated by maximum likelihood (details in text).**

the species (tips) values and the shape at the estimated position of the root (most recent common ancestor, MRCA) of the *Euvola* clade. These vectors were obtained using the full set of principal component scores (93 dimensions), which captured 100% of the observed shape variation. All pairwise angles between these vectors were then obtained, and the mean was calculated. Thus, MPA measures the relative direction traveled by species in the focal lineage away from the root, where a small mean pairwise angle signifies that the shape evolution exhibited by species in the *Euvola* clade has proceeded in a similar direction in morphospace.

The above generalization of Wood et al.'s procedure provides a quantitative measure of directional evolution in a phylogenetic context. To evaluate the observed pattern statistically, we adopted a phylogenetic simulation procedure similar to that of Pennell et al. (2015; also Boettiger et al. 2012) where the observed pattern was compared to patterns from simulated data obtained under alternative evolutionary scenarios. We compared the observed MPA to distributions obtained under two evolutionary scenarios: Brownian motion, and Brownian motion with a directional trend. The input parameters used for these simulations were obtained from the observed data. First, we obtained the standardized covariance matrix (i.e., correlation matrix) among traits for both the full dataset (Σ_{All}) and the *Euvola* clade (Σ_{Euv}). We then used the time-dated molecular phylogeny and Σ_{All} as the input covariance matrix to simulate 1000 data sets under a multivariate Brownian motion model of evolution (using "sim.char" in the R library *geiger* v. 2.0.6 (Harmon et al. 2008), starting at an arbitrary root value of 0 for all trait dimensions. For each dataset we obtained the MPA for the focal lineage, and generated a distribution of expected MPA values under Brownian motion.

For simulations where the focal lineage evolved via a directional trend, we used a modified version of *geiger*'s "sim.char," which incorporated the directional evolution capabilities of "fastBM" from the R library *phytools* v.0.5–10 (Revell 2012) into the multivariate framework that allowed for trait correlations. Specifically, we simulated 1000 datasets on the phylogeny for the sublineage (the focal group), using Σ_{Euv} as the input covariance matrix, and setting the mean of random normal generating function (μ: which generates the directional trend), to a positive value of 3. Because selection of the value of μ is not empirically derived, we additionally performed a sensitivity analysis across a range of values to determine the robustness of our biological conclusions relative to the choice of μ see Table S3). We also modified the "sim.char" function to take a multivariate root value, and the root MRCA for the *Euvola* clade from each BM simulated dataset was used as the root value for the directional simulation in that clade. Then the MPA value for each of these datasets were estimated, and the distribution of expected MPA values under Brownian motion with a directional trend was obtained. The observed MPA was then compared to both of these distributions to determine whether the observed pattern in morphospace was more consistent with one or the other alternative evolutionary scenario.

Finally, to evaluate the effect of within-species sampling error we performed an additional analysis where individuals were bootstrapped (100 times) within species and the MPA obtained

(see Denton and Adams 2015). This distribution of possible outcomes under within-species sampling error was then evaluated relative to possible outcomes under Brownian motion and Brownian motion with a directional trend.

All analyses (unless otherwise stated) were performed in R using the *geomorph* library v.3.0 (Adams and Otárola-Castillo 2013). The shape data, phylogeny, and all R computer scripts used for the analyses are available on Dryad (doi:10.5061/dryad.43548).

Results

We found significant differences in shells shape across life habits (D-PGLS, $F_{5,87} = 5.73$, $P < 0.001$), implying that these functional groups were phenotypically distinct in spite of shared evolutionary history. A principal components analysis of shape revealed that nearly 70% of the variation was described by the first two axes (Fig. 3). Furthermore, we found that the morphospace was partitioned by distinct shell shapes of these six life habits rather than by phylogenetic clades, as evidenced in the phylomorphospace (Fig. 3, Fig. S2). Thus morphological diversification of shell shape was predominantly due to functional diversification in the environment.

The free-living and byssal attaching scallops occupied most of the shape space and appeared to overlap greatly (including along PC3, which contributes 12.2%, see Fig. S2), implying there were many shared features of shell shape between these two life habits (Fig. 3). The majority of the ancestral states were estimated in the middle of this cluster, including the estimated position of the root ancestor. Branches among the byssal and free-living species, along with their inferred ancestors, were arranged in morphospace in a "bird's nest" configuration with many crisscrossing branches. From the length and direction of branches, it was evident that most closely related species of these life habits were phenotypically very different.

Emanating from the bird's nest of byssal-attaching and free-living species were long branches leading to species of the other life habits (Fig. 3); indicating that species of gliding, nestling, and cementing scallops independently traversed the morphospace in different directions away from the large cluster to occupy different areas on the periphery. This supported our finding from the D-PGLS that these life habit groups were phenotypically distinct. The trajectories of the branches from estimated ancestors implied that they evolved from species with shell shapes more similar to byssal-attaching or free-living species. For instance, the gliders evolved into an area of shape space defined by flat and circular valves with small auricles. In contrast, the nestling and cementing species were dorso-ventrally elongated with small auricles.

The phylogeny also revealed that a recessing life habit evolved twice in scallops (Fig. 2). The recessing species of the *Patinopecten* clade and *Euvola* clade both appear to have traversed morphospace away from the byssal/free-living cluster and shared a similar shape trend, which was described as a progressive flattening of the left valve leading to concavity at the extreme end of the trend (Fig. 4). Variation within the *Euvola* clade that is perpendicular to the direction of the trend and similar to variation along PC2 (Fig. 4) relates to changes in the size and shape of the auricles (overall positive values of PC2 corresponded to a small auricle, while negative PC2 values are large, dorsally expanded auricles).

Surprisingly, the phylomorphospace also revealed what appeared to be a distinct directional phylogenetic trend in the *Euvola* recessing clade (Fig. 4). Here, taxa were successively aligned in shape space, starting from the common ancestor of the Pectinidae, leading in an oblique direction along principal axes 1 and 2 (and 3, Fig. S2). This manifests in the phylomorphospace (e.g., Fig. 3) as a pattern of shape evolution that progresses further and further away from the common ancestor of the clade through apparently step-wise events (Fig. 4), with two exceptions: the two species (*E. papyraceum* and *A. pleuronectes*) that independently evolved the gliding habit in the *Euvola* clade have each broken away from the directional trend and traversed back to occupy a region with other gliding species. In support of this visual trend, we found that the shell shape of *Euvola clade* recessers is significantly different to that of all other species (D-PGLS, $F_{1,91} = 14.99$, $P < 0.001$), signifying that these species have dispersed to occupy a novel area of morphospace.

Using the mean pairwise angle approach described above, we found that the recessers of the *Euvola* clade displayed a consistent direction of evolutionary change in morphospace, with a low mean pairwise angle ($MPA_{obs} = 41.5°$). When this value was compared to what was expected under alternative evolutionary scenarios obtained from phylogenetic simulations, we found that the observed pattern did not fall within the distribution obtained under multivariate Brownian motion (Fig. 5). Specifically, the mean value, and in fact the entire distribution of MPA values obtained under Brownian motion, was considerably larger than the observed (mean MPA_{BM} from 1000 simulations $= 60.1°$), indicating markedly less consistency in the direction of shape evolution under Brownian motion than was observed in the *Euvola* clade. As such, there was little support for the hypothesis that the observed pattern was the result of simple Brownian motion.

By contrast, we found that the observed pattern was more similar to, and fell within, the distribution obtained from simulations using Brownian motion combined with a directional trend (Fig. 5). Under this evolutionary scenario, the direction of evolution among taxa was considerably more consistent, and the distribution of simulation outcomes was shifted more towards the observed MPA. Further, when alternative values of the strength of directional evolution (μ) were used, we found that this general pattern remained robust; namely, that the distribution of outcomes

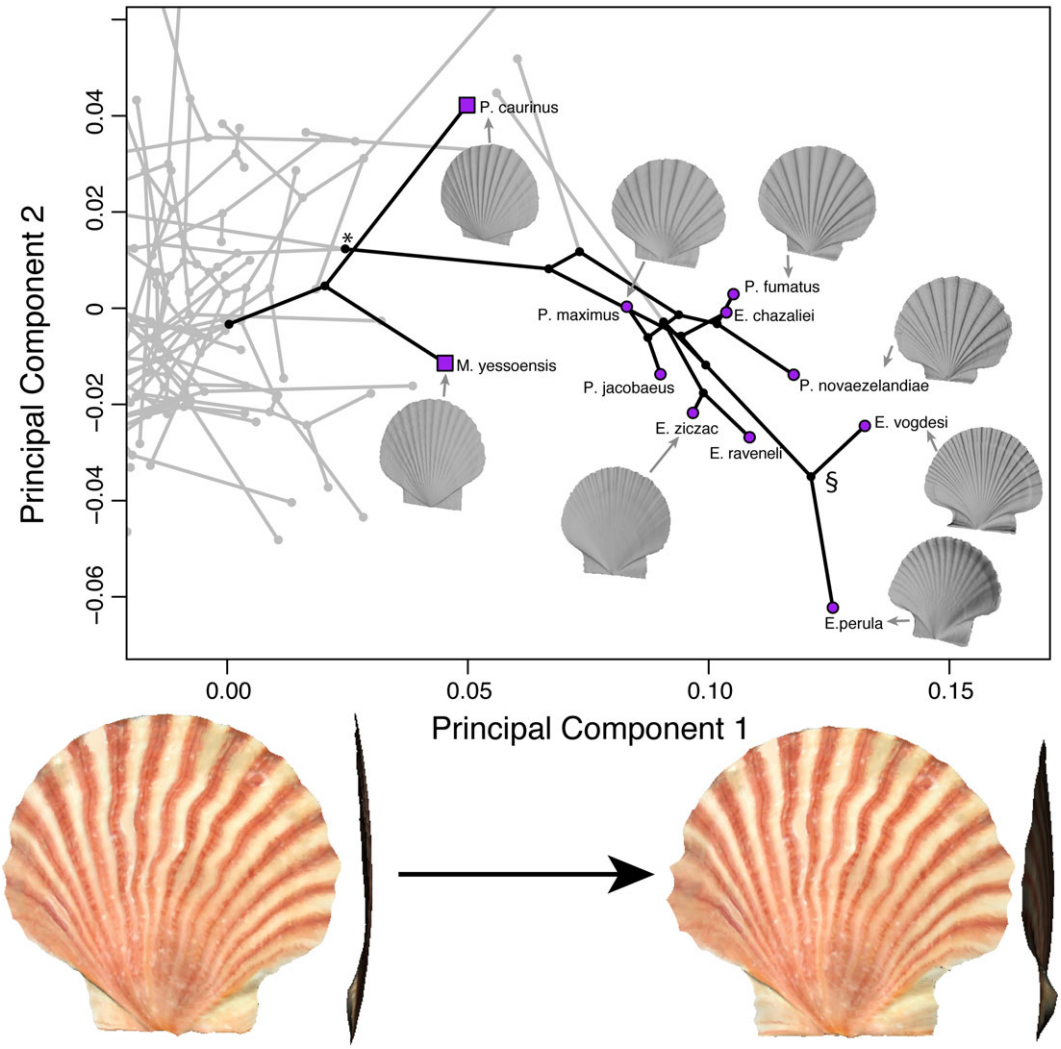

Figure 4. **Phylomorphospace showing the recesser species: the *Patinopecten* clade (squares) and *Euvola* clade (circles). Valves of representative species are shown. Below, the directional shape evolution is depicted from the estimated *Euvola* ancestor (*), a convex shell with flat auricles, to a descendant (common ancestor of *E. vogdesi* and *E. perula* §), a concave shell with concave auricles.**

from simulations under Brownian motion combined with a directional trend were more similar to the observed value than was the distribution obtained under only Brownian motion (Table S3, Fig. S3). Thus, from the phylogenetic simulations examined here, we found that the observed pattern was more consistent with the hypothesis of Brownian motion combined with a directional trend, as compared to an evolutionary scenario in which only Brownian motion was observed. Finally, bootstrap analyses evaluating the effect of within-species sampling error revealed that the observed patterns were robust to the effects of within-species sampling error (Fig. S4).

Discussion

Directional changes over macroevolutionary time are one of the most compelling evolutionary patterns observed in nature. In this study, we evaluated patterns of morphological evolution in 93 species of scallops within a phylogenetic context. We identified a striking pattern of apparent directional evolution in phylomorphospace involving a subset of nine closely related species. This subset, the *Euvola* clade, which is comprised primarily of recessing species of the *Euvola* and *Pecten* genera, occupied a distinct region of shape space; its taxa were distributed along a narrow, elliptical trajectory leading away from their progenitor, and have maintained a consistently narrow path through morphospace over time. We quantified this putative directional evolution using a phylogenetic generalization of methods for characterizing multivariate directional evolution in allochronic sequences, finding a consistent trend over time. Using phylogenetic simulations, we then compared this observed trend to what was expected under alternative evolutionary scenarios. This approach clearly demonstrated that the observed pattern differed from what was

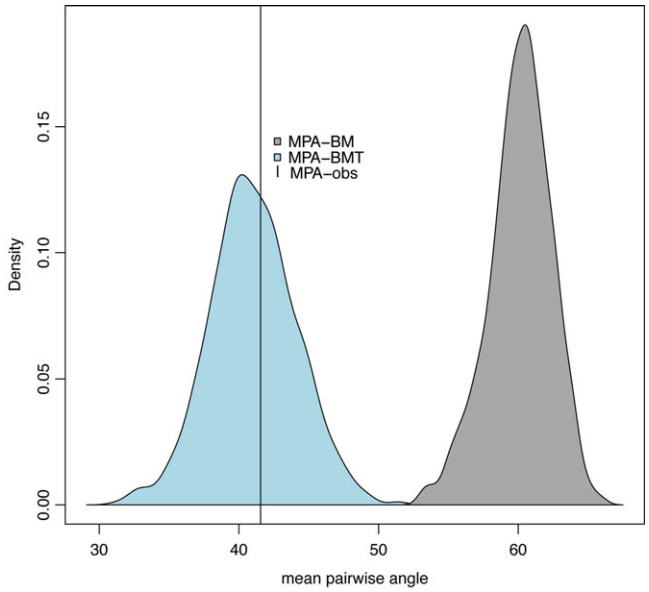

Figure 5. Histogram of the mean pairwise angle (MPA) observed in the *Euvola* recessers (MPA-obs), shown against the distribution of MPAs from simulations under Brownian motion (MPA-BM, grey) and Brownian motion with a directional trend (MPA-BMT, blue). Trend simulated using a strength of directional evolution ($\mu = 3$). 1000 simulations were performed under each. Angles shown in degrees (°). For other values of μ see supplementary materials.

expected under Brownian motion alone. Instead, the empirical data matched very closely to multivariate data simulated under BM with a strong trend of directional evolution in the focal subset. Thus, a consilience-based approach of discovery of a step-wise occupation of morphospace (Fig. 4) and simulation-based hypothesis testing (Fig. 5) enabled us to reject the hypothesis that these species entered a novel area of morphospace and diversified solely via Brownian motion. Rather, the observed pattern is shown to be consistent with what is expected under Brownian motion plus a directional trend (however we consider other possibly processes by which this pattern could manifest below).

We have shown that generally, recessing species of the *Euvola* clade occupy a distinct region of morphospace because the left valve (examined here) is substantially flatter than in other nonrecessing species. The auricles are consistently large in all *Euvola-Pecten* recessing species, which discriminates the flattened-valve morphology of recessers from that of gliding species (that have very small auricles, Fig. 3). Thus, the directional trend we identified in *Euvola-Pecten* recessing species corresponds to a morphological shift from a flattened valve to a distinctly concave valve in the most extreme recesser phenotype. The results obtained here suggest that shell morphology in recessing scallops is undergoing strong directional evolution along an environmental gradient, or shell shape is under some functional constraints. We recognize however, that the narrow, elongate spread may also suggest the *Euvola-Pecten* recessing species are evolving along an adaptive ridge, and thus an Ornstein-Uhlenbeck (OU) process with a single or multiple optima may also reasonably fit the data. However, the highly multidimensional data herein presently precludes such an analysis. Nevertheless, by comparing the phylomorphospace pattern of step-wise morphospace occupation along with the MPA is consistent with what is expected under a hypothesis of directional evolution.

The directional trend in valve morphology of the recessing species of the *Euvola* clade appears to coincide with the transition from an epifaunal to semiinfaunal existence. Based on ancestral state reconstruction of life habit (Alejandrino et al. 2011), the recessing behavior was derived from a free-living ancestor. Similarly, the reconstructed ancestral shape of the *Euvola* clade was within the morphospace of the free-living life habit. In free-living scallops, both left and right (upper and lower, respectively) valves are domed, and the degree of convexity of the right valve appears to be associated with shifts between open marine and shallow bay-sound environments, and the respective hydrodynamic regimes, over evolutionary time (Waller 1969). Recessers are "plano-convex" or "concavo-convex," meaning they have a convex lower valve and an upper valve (reported here) that is flattened or concave. Since both recessing and free-living species tend to be associated with substrates of small particle size (e.g., sand or sandy-mud) and have similar convexity in the lower valves (data not shown), shape of the upper valve may be more important for the recessing behavior. Thus, the directional trend identified here corresponds to a shift into new habitats, where the flat upper valve transitions to more concave shape. Further, these changes in the concavity of the upper valve may indicate performance differences among recessing species. For example, shell shape may affect the animal's ability to recess, anchor, or feed in substrates of different particle sizes (Baird 1958; Shumway et al. 1987) or habitats with different hydrodynamic regimes (Kirby-Smith 1972; Wildish et al. 1987; Pilditch and Grant 1999; Sakurai and Seto 2000; Moschino et al. 2015). Experimental functional morphological evidence in concavo-convex brachiopods also supports these hypotheses (Shiino and Suzuki 2011). As such, the evolutionary trend we see in the shell shape of *Euvola* and *Pecten* recessers may have played an important role in exploiting novel habitats or resources unavailable to nonrecessing species. Nevertheless, while recessers have been associated with substrates of small particle size (e.g., Mendo et al. 2014), there is little information on the specific habitat requirements for individual species. These data are necessary to investigate environmental factors that may correlate with the directional trend observed here. Because a directional trend in body shape would be an expected pattern if related lineages are found to consecutively occupy more specialized habitats, future work should test how shell shape or animal's position in a substrate affects performance (e.g., efficient recessing,

anchoring, feeding). These data examined in a comparative context may provide insight on the evolutionary relevance of the pattern of directional change observed in recessing scallop species.

Summary

We have demonstrated that for a subclade of taxa embedded in a larger phylogeny, directional trends in multivariate shape space can be obvious and striking within a phylogenetic context, despite the challenges of identifying such directional trends in univariate datasets. By using the phylomorphospace approach, a systematic, directional trend in morphological change aligned with speciation events can be easily visualized. Coupling this result with a straightforward test for whether the phenotypic dispersion of species evolved consistently in one direction, and phylogenetic simulation of multivariate data under different evolutionary scenarios, we were able to ascertain a putative directional trend in shell shape of recesser scallops. In scallops, this directional trend is explained as a putative adaptation to fast flowing water in recessing species, where recessing may be beneficial to prevent being washed away as well as maximize nutrient uptake in fast currents. Furthermore, our study highlights the advantages to studying complex traits with multivariate tools, and retaining high-dimensional data for evolutionary analyses, particularly for questions relating to modes of evolution. Indeed, other recent advances in the phylogenetic comparative toolkit have facilitated the examination of additional macroevolutionary patterns in complex, multidimensional traits. With these recent tools, one may now evaluate the degree of phylogenetic signal in multivariate traits (Adams 2014a), estimate their rates of phenotypic evolution (Adams 2014c), and examine evolutionary correlations for high-dimensional data (Adams 2014b; Adams and Collyer 2015). Our approach thus builds on this growing body of multivariate macroevolutionary methods by enabling the analysis of directional trends in multivariate traits; thereby extending the phylogenetic comparative toolkit in yet another dimension.

ACKNOWLEDGMENTS

We are very grateful for the assistance and loans provided by the staff of museums and research institutions, especially J. McLean and L. Groves of the Natural History Museum of Los Angeles County; G. Paulay and J. Slapcinsky of the Florida Museum of Natural History; E. Shea, N. Aziz and L. Skibinski of the Delaware Museum of Natural History; S. Morrison and C. Whisson of the Western Australian Museum, Perth; E. Strong, T. Nickens, P. Greenhall and T. Walter at the Smithsonian Institution; E. Lazo-Wasem at the Yale Peabody Museum of Natural History; G.T. Watters at the Museum of Biological Diversity, Columbus; P. Bouchet and P. Maestrati at the Muséum National d'Histoire Naturelle, Paris; A. Baldinger at the Museum of Comparative Zoology, Harvard; M. Siddall and S. Lodhi at the American Museum of Natural History; R. Bieler and J. Gerber at the Field Museum of Natural History, Chicago; R. Kawamoto at the Bernice Pauahi Bishop Museum, E. Kools at the California Academy of Sciences; A. Bogan and J. Smith at the North Carolina Museum of Natural Sciences; L. Groves at the Natural History Museum of Los Angeles County. Organization and collection of molecular and morphological data were aided by the team of undergraduate researchers: K. Boyer, D. Brady, K. Cain, G. Camacho, N. Dimenstein, C. Figueroa, A. Flander, A. Frakes, C. Grula, M. Hansel, M. Harmon, S. Hofmann, J. Kissner, N. Laurito, N. Lindsey, S. Luchtel, C. Michael, V. Molian, A. Oake, J. Rivera, H. Sanders, M. Steffen and C. Wasendorf. Financial support was provided by a Lerner-Gray Marine Research Grant from the American Museum of Natural History [to A.A.] and the United States National Science Foundation [DEB-1118884 to J.M.S. and D.C.A., and DEB-1257287 to D.C.A.]. Finally, we are grateful to G. Hunt for critical feedback that greatly improved the manuscript. We declare no conflict of interest.

DATA ARCHIVING

The doi for our data is 10.5061/dryad.43548.

LITERATURE CITED

Adams, D. C. 2014a. A generalized K statistic for estimating phylogenetic signal from shape and other high-dimensional multivariate data. Syst. Biol. 63:685–697.

———. 2014b. A method for assessing phylogenetic least squares models for shape and other high-dimensional multivariate data. Evolution 68:2675–2688.

———. 2014c. Quantifying and comparing phylogenetic evolutionary rates for shape and other high-dimensional phenotypic data. Syst. Biol. 63:166–177.

Adams, D. C., and M. L. Collyer. 2009. A general framework for the analysis of phenotypic trajectories in evolutionary studies. Evolution 63:1143–1154.

———. 2015. Permutation tests for phylogenetic comparative analyses of high-dimensional shape data: what you shuffle matters. Evolution 69:823–829.

Adams, D. C., and E. Otárola-Castillo. 2013. geomorph: an R package for the collection and analysis of geometric morphometric shape data. Methods Ecol. Evol. 4:393–399.

Adams, D. C., F. J. Rohlf, and D. E. Slice. 2013. A field comes of age: geometric morphometrics in the 21st century. Hystrix-Italian J. Mammal. 24:7–14.

Alejandrino, A., L. Puslednik, and J. M. Serb. 2011. Convergent and parallel evolution in life habit of the scallops (Bivalvia: Pectinidae). BMC Evol. Biol. 11:164.

Alroy, J. 1998. Cope's rule and the dynamics of body mass evolution in North American fossil mammals. Science 280:731–734.

———. 2000. Understanding the dynamics of trends within evolving lineages. Paleobiology 26:319–329.

Baird, R. H. 1958. On the swimming behaviour of scallops (*Pecten maximus* L.). Proc. Malacol. Soc. Lond. 33:67–71.

Bales, G. S. 1996. Heterochrony in brontothere horn evolution: allometric interpretations and the effect of life history scaling. Paleobiology 22:481–495.

Bergmann, P. J., J. J. Meyers, and D. J. Irschick. 2009. Directional evolution of stockiness coevolves with ecology and locomotion in lizards. Evolution 63:215–227.

Boettiger, C., G. Coop, and P. Ralph. 2012. Is your phylogeny informative? Measuring the power of comparative methods. Evolution 66:2240–2251.

Bookstein, F. L. 1987. Random walk and the existence of evolutionary rates. Paleobiology 13:446–464.

———. 1988. Random walk and the biometrics of morphological characters. Pp. 369–398 *in* M. Hecht, and B. Wallace, eds. Evol. Biol. Vol. 23. Springer, USA.

Bookstein, F. L. 1991. Morphometric tools for landmark data: geometry and biology. Cambridge Univ. Press, New York.

———. 2013. Random walk as a null model for high-dimensional morphometrics of fossil series: geometrical considerations. Paleobiology 39:52–74.

Collyer, M. L., and D. C. Adams. 2013. Phenotypic trajectory analysis: comparison of shape change patterns in evolution and ecology. Hystrix 24:75–83.

Cope, E. D. 1896. The primary factors of organic evolution. The Open Court Publishing Company, Chicago.

Denton, J. S. S., and D. C. Adams. 2015. A new phylogenetic test for comparing multiple high-dimensional evolutionary rates suggests interplay of evolutionary rates and modularity in lanternfishes (Myctophiformes; Myctophidae). Evolution 69:2425–2440.

Drummond, A. J., and A. Rambaut. 2007. BEAST: Bayesian evolutionary analysis by sampling trees. BMC Evol. Biol. 7:214.

Fortey, R. A., and R. M. Owens. 1990. Evolutionary trends in invertebrates: trilobites. Pp. 121–142 *in* J. A. McNamara, ed. Evolutionary trends. Arizona Univ. Press, Tucson.

Garland Jr, T., and A. R. Ives. 2000. Using the past to predict the present: confidence intervals for regression equations in phylogenetic comparative methods. Am. Nat. 155:346–364.

Gould, S. J. 1988. Trends as changes in variance: a new slant on progress and directionality in evolution. J. Paleontol. 62:319–329.

Gunz, P., P. Mitterocker, and F. L. Bookstein. 2005. Semilandmarks in three dimensions. Pp. 73-98 *in* D. E. Slice, ed. Modern morphometrics in physical anthropology. Kluwer Academic/Plenum Publishers, New York.

Harmon, L. J., J. T. Weir, C. D. Brock, R. E. Glor, and W. Challenger. 2008. GEIGER: investigating evolutionary radiations. Bioinformatics 24:129–131.

Heim, N. A., M. L. Knope, E. K. Schaal, S. C. Wang, and J. L. Payne. 2015. Cope's rule in the evolution of marine animals. Science 347:867–870.

Hone, D. E., and M. J. Benton. 2005. The evolution of large size: how does Cope's rule work? Trends Ecol. Evol. 20:4–6.

Hopkins, M. J. 2016. Magnitude versus direction of change and the contribution of macroevolutionary trends to morphological disparity. Biol. J. Linn. Soc. 118:116–130.

Hopkins, M. J., and S. Lidgard. 2012. Evolutionary mode routinely varies among morphological traits within fossil species lineages. Proc. Natl. Acad. Sci. USA 109:20520–20525.

Hunt, G. 2006. Fitting and comparing models of phyletic evolution: random walks and beyond. Paleobiology 32:578–601.

———. 2007. The relative importance of directional change, random walks, and stasis in the evolution of fossil lineages. Proc. Natl. Acad. Sci. USA 104:18404–18408.

Kearse, M., R. Moir, A. Wilson, S. Stones-Havas, M. Cheung, S. Sturrock, S. Buxton, A. Cooper, S. Markowitz, C. Duran, T. Thierer, B. Ashton, P. Mentjies, and A. Drummond. 2012. Geneious Basic: an integrated and extendable desktop software platform for the organization and analysis of sequence data. Bioinformatics 28:1647–1649.

Kirby-Smith, W. W. 1972. Growth of the bay scallop: the influence of experimental water currents. J. Exp. Mar. Biol. Ecol. 8:7–18.

Klingenberg, C. P., and W. Ekau. 1996. A combined morphometric and phylogenetic analysis of an ecomorphological trend: pelagization in Antarctic fishes (Perciformes: Nototheniidae). Biol. J. Linn. Soc. 59:143–177.

Klingenberg, C. P., and L. R. Monteiro. 2005. Distances and directions in multidimensional shape spaces: implications for morphometric applications. Syst. Biol. 54:678–688.

Knouft, J. H., and L. M. Page. 2003. The evolution of body size in extant groups of North American freshwater fishes: speciation, size distributions, and Cope's rule. Am. Nat. 161:413–421.

MacFadden, B. J. 1986. Fossil horses from "Eohippus" (*Hyracotherium*) to *Equus*: scaling, Cope's law, and the evolution of body size. Paleobiology 12:355–369.

———. 2005. Fossil horses—evidence for evolution. Science 307:1728–1730.

McKinney, M. L. 1990. Classifying and analysing evolutionary trends. Pp. 28-58 *in* J. A. McNamara, ed. Evolutionary trends. Arizona Univ. Press, Tucson.

McNamara, K. J. 2006. Evolutionary trends. Encyclopedia of life sciences. John Wiley & Sons Ltd., Chichester.

McShea, D. W. 1994. Mechanisms of large-scale evolutionary trends. Evolution 48:1747–1763.

Mendo, T., J. M. Lyle, N. A. Moltschaniwskyj, S. R. Tracey, and J. M. Semmens. 2014. Habitat characteristics predicting distribution and abundance patterns of scallops in D'Entrecasteaux Channel, Tasmania. Plos ONE 9:e85895.

Mitteroecker, P., and P. Gunz. 2009. Advances in geometric morphometrics. Evol. Biol. 36:235–247.

Moschino, V., M. Bressan, L. Cavaleri, and L. Da Ros. 2015. Shell-shape and morphometric variability in *Mytilus galloprovincialis* from micro-tidal environments: responses to different hydrodynamic drivers. Mar. Ecol. 36:1440–1453.

Osborn, H. F. 1929. The titanotheres of ancient Wyoming, Dakota, and Nebraska. Vol 55.

Pagel, M. 1997. Inferring evolutionary processes from phylogenies. Zool. Scr. 26:331–348.

Pennell, M. W., R. G. FitzJohn, W. K. Cornwell, and L. J. Harmon. 2015. Model adequacy and the macroevolution of Angiosperm functional traits. Am. Nat. 186:E33–E50.

Pilditch, C. A., and J. Grant. 1999. Effect of variations in flow velocity and phytoplankton concentration on sea scallop (*Placopecten magellanicus*) grazing rates. J. Exp. Mar. Biol. Ecol. 240:111–136.

Poulin, R. 2005. Evolutionary trends in body size of parasitic flatworms. Biol. J. Linn. Soc. 85:181–189.

R Development Core Team. 2014. R: a language and environment for statistical computing. Vienna, Austria.

Raup, D. M. 1966. Geometric analysis of shell coiling: general problems. J. Paleontol. 40:1178–1190.

Rencher, A. C., and W. F. Christensen. 2012. Methods of multivariate analysis. 3rd ed. John Wiley & Sons, Inc., Hoboken, NJ.

Rensch, B. 1948. Histological changes correlated with evolutionary changes of body size. Evolution 2:218–230.

Revell, L. J. 2012. phytools: an R package for phylogenetic comparative biology (and other things). Methods Ecol. Evol. 3:217–223.

Revell, L. J., M. A. Johnson, J. A. Schulte, J. J. Kolbe, and J. B. Losos. 2007. A phylogenetic test for adaptive convergence in rock-dwelling lizards. Evolution 61:2898–2912.

Rohlf, F. J. 2002. Geometric morphometrics and phylogeny. Pp. 175-193 *in* N. MacLeod, and P. L. Forey, eds. Morphology, shape and phylogeny. Francis & Taylor, London.

Rohlf, F. J., and D. Slice. 1990. Extensions of the Procrustes method for the optimal superimposition of landmarks. Syst. Zool. 39:40–59.

Roopnarine, P. D., G. Byars, and P. Fitzgerald. 1999. Anagenetic evolution, stratophenetic patterns, and random walk models. Paleobiology 25:41–57.

Sakurai, I., and M. Seto. 2000. Movement and orientation of the Japanese scallop *Patinopecten yessoensis* (Jay) in reponse to water flow. Aquaculture 181:269–279.

Scannella, J. B., D. W. Fowler, M. B. Goodwin, and J. R. Horner. 2014. Evolutionary trends in *Triceratops* from the Hell Creek formation, Montana. Proc. Natl. Acad. Sci. USA 111:10245–10250.

Schluter, D., T. D. Price, A. O. Mooers, and D. Ludwig. 1997. Likelihood of ancestor states in adaptive radiation. Evolution 51:1699–1711.

Serb, J. M., A. Alejandrino, E. Otárola-Castillo, and D. C. Adams. 2011. Morphological convergence of shell shape in distantly related scallop species (Mollusca: Pectinidae). Zool. J. Linn. Soc. 163:571–584.

Sheets, H. D., and C. Mitchell. 2001. Why the null matters: statistical tests, random walks and evolution. Genetica 112–113:105–125.

Sheldon, P. R. 1987. Parallel gradualistic evolution of Ordovician trilobites. Nature 330:561–563.

Shiino, Y., and Y. Suzuki. 2011. The ideal hydrodynamic form of the concavo-convex productide brachiopod shell. Lethaia 44:329–343.

Shumway, S., R. Selvin, and D. Schick. 1987. Food resources related to habitat in the scallop *Placopecten magellanicus* (Gmelin, 1791): a qualitative study. J. Shellfish Res. 6:89–95.

Sidlauskas, B. 2008. Continuous and arrested morphological diversification in sister clades of characiform fishes: a phylomorphospace approach. Evolution 62:3135–3156.

Simpson, G. G. 1944. Tempo and mode in evolution. Columbia Univ. Press, New York.

Stanley, S. M. 1970. Relation of shell form to life habits of the Bivalvia (Mollusca). Geol. Soc. Am. Memoirs 125:1–296.

Stayton, C. T. 2006. Testing hypotheses of convergence with multivariate data: morphological and functional convergence among herbivorous lizards. Evolution 60:824–841.

Talavera, G., and J. Castresana. 2007. Improvement of phylogenies after removing divergent and ambiguously aligned blocks from protein sequence alignments. Syst. Biol. 56:564–577.

Verdú, M. 2006. Tempo, mode and phylogenetic associations of relative embryo size evolution in angiosperms. J. Evol. Biol. 19:625–634.

Vermeij, G. J. 1987. Evolution and escalation. Princeton Univ. Press., Princeton.

Wagner, P. J. 1996. Contrasting the underlying patterns of active trends in morphologic evolution. Evolution 50:990–1007.

Waller, T. R. 1969. The evolution of the *Argopecten gibbus* stock (Mollusca: Bivalvia), with emphasis on the Tertiary and Quaternary species of eastern North America. Memoir (The Paleontological Society) 3: i–125.

Wildish, D., D. Kristmanson, R. Hoar, A. DeCoste, S. McCormick, and A. White. 1987. Giant scallop feeding and growth responses to flow. J. Exp. Mar. Biol. Ecol. 113:207–220.

Wood, A., M. L. Zelditch, A. N. Rountrey, P. D. Gingerich, and H. D. Sheets. 2007. Multivariate stasis in the dental morphology of the Paleocene-Eocene condylarth *Ectocion*. Paleobiology 33:248–260.

Associate Editor: C. Ané
Handling Editor: R. Shaw

Supporting Information

Additional Supporting Information may be found in the online version of this article at the publisher's website:

Figure S1. Chronogram of 143 scallop species.
Figure S2. Phylomorphospace of average shape for 93 species using PC1 and PC3, colored by habit group (same as figure 2).
Figure S3. Histogram of the mean pairwise angle (MPA) observed in the *Euvola* recessers (MPA-obs), shown against the distribution of MPAs from simulations under Brownian motion (MPA-BM, grey) and Brownian motion with a directional trend (MPA-BMT, blue).
Figure S4. Histogram of the mean pairwise angles (MPA) from a bootstrap analysis to evaluate the effect of within-species sampling error.
Table S1. Morphometric data were available for 93 species comprising six life habits.
Table S2. Genbank accession numbers for 143 specimens included in the molecular phylogeny.
Table S3. Sensitivity simulations using different strengths of directional evolution (μ, from 2.1 to 3.5).